COLLECTIVE EFFECTS ISSUES FOR FCC-ee

M. Migliorati[1*], E. Belli[1,2], G. Castorina[3], S. Persichelli[4], B. Spataro[3], M. Zobov [3]
[1] University of Rome 'La Sapienza' and INFN Sez. Roma1, Rome, Italy
[2] CERN, Geneva, Switzerland
[3] INFN-LNF - Frascati - Roma - Italy
[4] LBNL - Berkeley - CA - USA

Abstract

The Future Circular Collider study, hosted by CERN to design post-LHC particle accelerator options in a worldwide context, represents a great challenge under several aspects, which require R&D on beam dynamics and new technologies. One very critical point is represented by collective effects, generated by the interaction of the beam with self-induced electromagnetic fields, called wake fields, which could produce beam instabilities, thus reducing the machines performance and limiting the maximum stored current. It is therefore very important to be able to predict these effects and to study in detail potential solutions to counteract them. In this paper the resistive wall and some other important geometrical sources of impedance for the FCC electron-positron accelerator are identified and evaluated, and their impact on the beam dynamics, which could lead to unwanted instabilities, is discussed.

INTRODUCTION

The new CERN project, called High Luminosity LHC [1], aims to increase the number of collisions accumulated in the experiments by a factor of ten from 2024 onwards. While the project is well defined for the next two decades, CERN has started an exploratory study for a future long-term project based on a new generation of circular colliders with a circumference of about 100 km. The Future Circular Collider (FCC) study [2] has been undertaken to design a high energy proton-proton machine (FCC-hh), capable of reaching unprecedented energies in the region of 100 TeV, and a high-luminosity e+e- collider (FCC-ee), serving as Z, W, Higgs and top factory, with luminosities ranging from about 10^{34} to 10^{36} cm^{-2}s^{-1} per collision point as a potential intermediate step towards the realization of the hadron facility. The design of the lepton collider complex will be based on the same infrastructure as the hadron collider.

At high beam intensity, necessary to reach the high luminosity foreseen for FCC-ee, the electromagnetic fields, self-generated by the beam interacting with its immediate surroundings and known as wake fields [3], act back on the beam, perturbing the external guiding fields and the beam dynamics. Under unfavorable conditions, the perturbation on the beam further enhances the wake fields; the beam-surroundings interaction then can lead to a reduction of the machine performance and, in some cases, also to instabilities.

* mauro.migliorati@uniroma1.it

ISBN 978-3-95450-187-8

The theory of collective beam instabilities induced by the wake fields is a broad subject and it has been assessed over many years by the work of many authors, such as F. Sacherer [4], A. W. Chao [5], J. L. Laclare [6], B. Zotter [7], C. Pellegrini [8], M. Sands [9] and others [10].

To simplify the study of collective effects, in general it is convenient to distinguish between short range wake fields, which influence the single bunch beam dynamics, and long range wake fields, where high quality factor resonant modes excited by a train of bunches can last for many turns exciting, under some conditions, coupled bunch instabilities. In both cases the bunch motion is considered as a sum of coherent oscillation modes perturbed by these wake fields.

In this paper we will focus on the FCC-ee collective effects induced by wake fields. In particular we will first evaluate the wake fields induced by the finite resistivity of the beam vacuum chamber (resistive wall). Due to the 100 km length of the beam pipe, the resistive wall plays a non negligible role among the sources of wake fields for this accelerator, and the choice of the pipe geometry, material, and dimensions is particularly important. We then discuss the collective effects induced by the resistive wall for both the short range and long range wake fields, and for both longitudinal and transverse planes. For some instabilities we will resort to the linear theory, while for other cases and for more accurate predictions, we need to use simulation codes.

We finally dedicate the last part of the paper to other important sources of wake fields, such as the RF system, the synchrotron radiation absorbers, and smooth transitions, in order to reduce their impact on the beam dynamics. Finally, concluding remarks and outlook will end the paper.

For reference we report in Table 1 the list of beam parameters for the two lowest energies that we have used for evaluating the effects of wake fields on the beam dynamics. At the 45.6 GeV energy, two options are foreseen, with the same total beam current and a different bunch spacing, 7.5 ns and 2.5 ns. It is important to observe that the 7.5 ns option is more critical, from the single bunch point of view, with respect to the 2.5 ns option, having a triple bunch current and a shorter bunch length.

RESISTIVE WALL WAKE FIELDS, IMPEDANCES, AND EFFECTS ON BEAM DYNAMICS

The electromagnetic interaction of the beam with the surrounding vacuum chamber, due to its finite resistivity, produces unavoidable wake fields, which, for FCC-ee, result

Table 1: Parameter List used to Evaluate the Beam Dynamics Effects of Wake Fields

Circumference (km)	100	100	100
Beam energy (GeV)	45.6	45.6	80
Beam current (mA)	1450	1450	152
Mom. compaction (10^{-5})	0.7	0.7	0.7
Betatron tune	350	350	350
RF frequency (MHz)	400	400	400
Bunch spacing (ns)	7.5	2.5	50
RF voltage (GV)	0.4	0.2	0.8
Bunch length (mm)*	1.2	1.6	2.0
Energy spread (10^{-3})*	0.37	0.37	0.65
Synchrotron tune	0.036	0.025	0.037
Bunches/beam	30180	91500	5260
Bunch population (10^{11})	1.0	0.33	0.6

* without beamstrahlung (no collision, worst case)

to be of particular importance. If we consider a beam pipe with circular cross section and a single material of infinite thickness, the longitudinal monopolar ($m = 0$) coupling impedance is given by [11]

$$\frac{Z_{||}(\omega)}{C} = \frac{Z_0 c}{\pi} \frac{1}{[1 + i\,\mathrm{sgn}(\omega)]\, 2bc\sqrt{\frac{\sigma_c Z_0 c}{2|\omega|}} - ib^2\omega} \quad (1)$$

and the transverse dipolar ($m = 1$) one by

$$\frac{Z_{\perp}(\omega)}{C} = \frac{Z_0 c^2}{\pi} \frac{2}{[\mathrm{sgn}(\omega) + i]\, b^3 c\sqrt{2\sigma_c Z_0 c\,|\omega|} - ib^4\omega^2} \quad (2)$$

where C is the machine circumference, Z_0 the vacuum impedance, c the speed of light, b the pipe radius, and σ_c the material conductivity. The above expressions are valid in a frequency range defined by

$$\frac{\chi c}{b} \ll \omega \ll \frac{c\chi^{-1/3}}{b} \quad (3)$$

with $\chi = 1/(Z_0\sigma_c c b)$. The corresponding wake functions are given by [12]

$$\frac{w_{||}(z)}{C} = \frac{4Z_0 c}{\pi b^2}\left[\frac{e^{-z/s_0}}{3}\cos\left(\frac{\sqrt{3}z}{s_0}\right) - \frac{\sqrt{2}}{\pi}\int_0^{\infty} dx \frac{x^2 e^{-zx^2/s_0}}{x^6 + 8}\right] \quad (4)$$

and

$$w_{\perp}(z) = \frac{2}{b^2}\frac{dw_{||}(z)}{dz} \quad (5)$$

with $z > 0$ and $s_0 = \left[2b^2/(Z_0\sigma_c)\right]^{1/3}$.

By considering a beam pipe of 35 mm of radius made by copper (conductivity of about 5.9e7 S/m) or aluminium (conductivity of about 3.8e7 S/m), eqs. (1) and (2) are valid in a very large range of frequency. In addition, it is important to observe that the last term in the denominator of eqs. (1) and (2) is negligible up to high frequencies, giving then the possibility to easily evaluate the scale of the impedance with the pipe radius. Indeed the longitudinal impedance is inversely proportional to the beam pipe radius, and the transverse one to the inverse of the third power of b. This scaling can be used to find a compromise for the pipe geometry. By reducing the radius it is possible to reduce the power required for the magnets, but this would increase in particular the coupling impedance and then reduce transverse instability thresholds.

The discussion on the vacuum chamber shape and material choice can be found in ref. [13]. In the following, for the beam dynamics studies, we will consider a circular beam pipe having 35 mm inner radius with three layers [14], a first layer of aluminium of 4 mm, then 6 mm of dielectric and finally iron with resistivity of 10^{-7} Ωm. In this case, the impedance has been evaluated with the code Impedance-Wake2D [15]. Even if the above equations are valid only for a single thick layer, for which the skin depth is much smaller than the wall thickness, the difference with respect to the code results starts to show up only below very low frequency. As a conclusion we can say that all the considerations derived from eqs. (1) and (2) are essentially valid also for the multilayer case.

Fig. 1 shows the total transverse and longitudinal resistive wall impedance as a function of frequency. This impedance is used in the following section for evaluating the resistive wall effect on beam dynamics.

Single Bunch Effects

One important effect of the resistive wall on the single bunch dynamics is related to the transverse mode coupling instability, or strong head tail instability [5]. The frequencies of the coherent modes are here calculated with DELPHI [15] code, which considers Laguerre polynomials. In Fig. 2 we show the real part of the frequency (tune shift) of the first two radial coherent oscillation modes, with the azimuthal number going from -2 to 2, as a function of the bunch population for 45.6 GeV, 2.5 ns of bunch spacing, and 80 GeV. As expected, the worst scenario is at the lowest energy, where we find an instability threshold that is a factor of about 6 higher than the nominal bunch population. However, if we consider the 7.5 ns bunch spacing case, the scenario can be worse due to the higher bunch current and lower bunch length. The higher energy cases, not shown here, give higher thresholds. In this situation we can see that, if other contributions to the transverse impedance do not exceed the resistive wall, we have a good margin of safety for this kind of instability. However, a more detailed study of transverse mode coupling instability with a more detailed transverse impedance is necessary.

For what concerns the longitudinal beam dynamics, one main problem caused by the resistive wall is related to the longitudinal potential well distortion and the evaluation of the microwave instability threshold. The microwave insta-

ISBN 978-3-95450-187-8

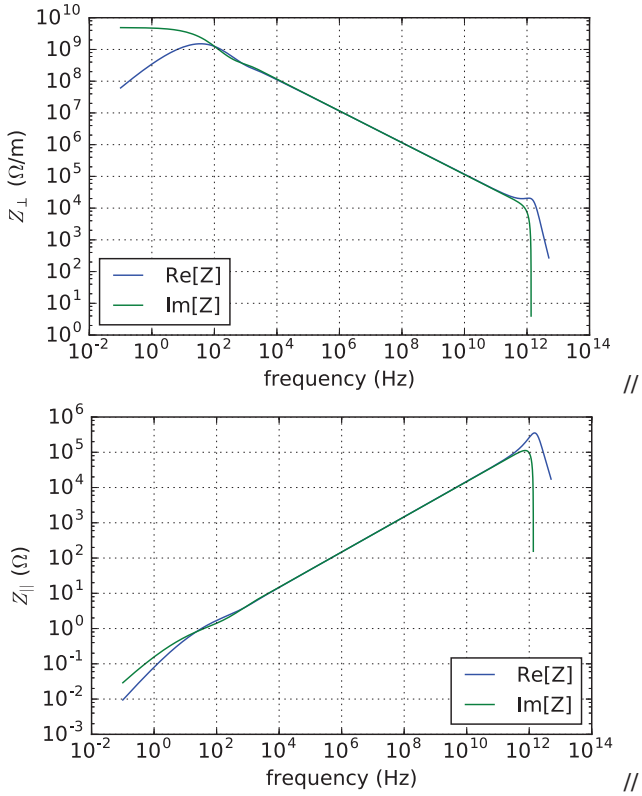

Figure 1: Real and imaginary part of transverse (top) and longitudinal (bottom) impedance of resistive wall as a function of frequency.

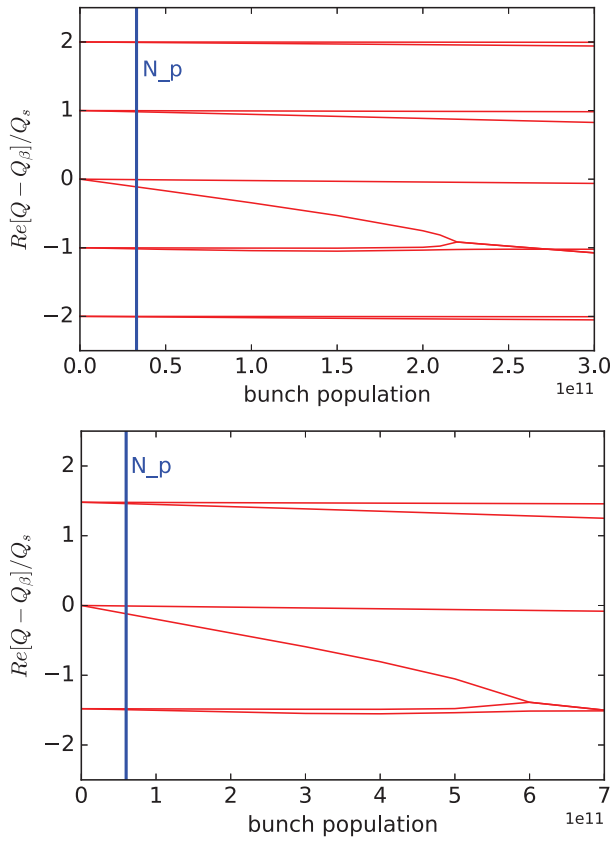

Figure 2: Real part of the frequency of the first coherent oscillation modes as a function of bunch population for the 45.6 GeV case (top) and the 80 GeV case (bottom).

bility does not produce a bunch loss, but the consequent longitudinal emittance increase and possible bunch internal oscillations that cannot be counteracted by a feedback system, make the microwave instability an effect that has to be studied with care. In addition to that, there are no reliable analytical expressions that can be used to easily evaluate the instability threshold. For these reasons we have performed a series of simulations by using a tracking code, which we refer here as SBSC [16], initially developed to study the longitudinal beam dynamics in DAΦNE damping and main rings [17], and successively developed and adapted to other machines [18].

In Fig. 3 in red and blue we show the wake potentials of 2 mm and 4 mm Gaussian bunches as given by the equation [19]

$$W_{||}(z) = \int_{-\infty}^{\infty} \lambda(z')w_{||}(z-z')dz' = \frac{cC}{8\sqrt{2}\pi b\sigma_z^{3/2}}\sqrt{\frac{Z_0}{\sigma_c}}F(z/\sigma_z) \quad (6)$$

with

$$F(x) = |x|^{3/2}e^{-x^2/4}\left(I_{1/4} - I_{-3/4} \pm I_{-1/4} \mp I_{3/4}\right) \quad (7)$$

where I_n are the modified Bessel functions, the upper signs in eq. (7) are for positive z, $\lambda(z)$ is the longitudinal distribution function, and $w_{||}(z)$ is the wake function given by eq. (4).

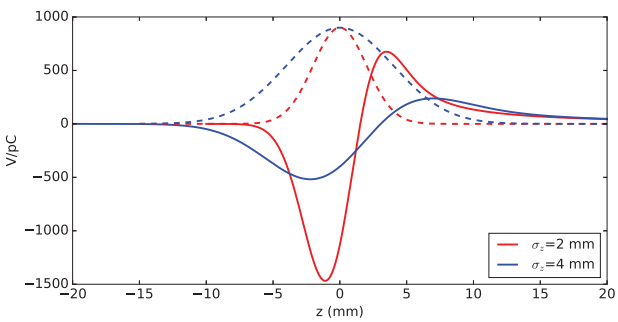

Figure 3: Resistive wall longitudinal wake potentials of 2 mm and 4 mm Gaussian bunches.

In order to perform a test of the code, and to evaluate the effect of the resistive wall on the longitudinal beam dynamics, we have first solved the Haïssinski integral equation [20], which is able to predict the bunch length and the distortion from a Gaussian distribution for intensities below the microwave instability threshold. The equation can be written as

$$\lambda(z) = \lambda_0 \exp\left[\frac{1}{E_0\eta\sigma_{\varepsilon 0}^2}\Psi(z)\right] \quad (8)$$

ISBN 978-3-95450-187-8

with λ_0 a normalization constant, E_0 the collider energy, η the slippage factor, $\sigma_{\varepsilon 0}$ the natural RMS energy spread, and

$$\Psi(z) = \frac{1}{C}\int_0^z [eV_{RF}(z') - U_0]\,dz' - \frac{e^2 N_p}{C}\int_0^z dz' \int_{-\infty}^{z'} \lambda(z'')w_{||}(z'-z'')dz'' \,. \quad (9)$$

where V_{RF} represents the total RF voltage, U_0 the energy lost per turn due to the synchrotron radiation, and N_p the bunch population.

The bunch shapes for different bunch populations at the lowest energy of 45.6 GeV for 2.5 ns bunch spacing are shown in Fig. 4.

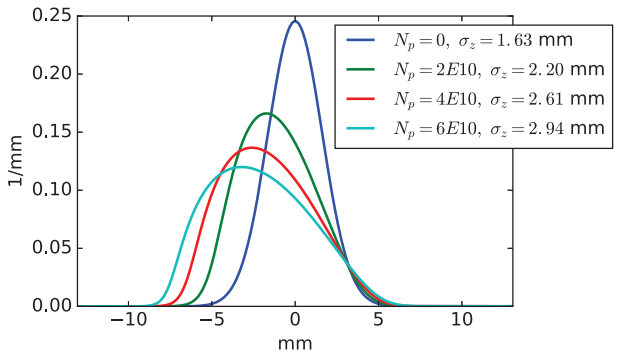

Figure 4: Longitudinal distribution for different bunch population as given by Haïssinski equation.

The bunch length is about 2.4 - 2.5 mm at the nominal current, but we have to remind that only the resistive wall effect has been taken into account for the moment. For the three shown bunch populations the tracking code gives exactly the same distribution.

The potential well distortion theory described by the Haïssinski equation predicts a bunch length increasing with current and a constant energy spread up to a given threshold, called microwave instability threshold, above which also the energy spread increases. In the microwave instability regime, even if the bunch is not lost, it could be characterized by internal turbulent motion which would compromise the machine performances. Several papers have been written to determine the microwave instability threshold [21]. In particular, in ref. [22], the microwave instability due to the resistive wall wake fields was analyzed giving a criterion for the threshold evaluation. Applied to the FCC-ee case, it gives a threshold value of $N_p = 8.1 \times 10^{10}$, a factor slightly higher than 2 with respect to the nominal bunch population for 2.5 ns bunch spacing.

This value can be compared with the results of the tracking code. From Fig. 5, where we represented the RMS energy spread given by the code as a function of the bunch population, we can see that the energy spread starts to increase at about $8 - 10 \times 10^{10}$. This is in a good agreement with the above analytical estimate. Even if there is a margin of safety for the 2.5 ns bunch spacing, for the 7.5 ns case, the nominal bunch current is found in a weak microwave instability regime.

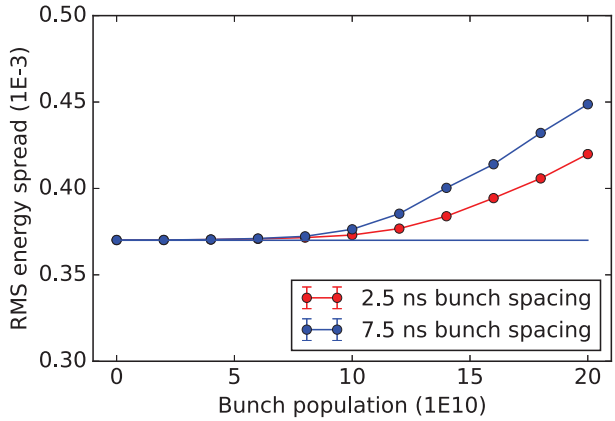

Figure 5: RMS energy spread as a function of bunch population given by the simulation code with only the resistive wall impedance for 2.5 ns and 7.5 ns bunch spacing.

As a further check of the tracking code results, a Vlasov-Fokker-Planck solver [23] has also been used for 2.5 ns bunch spacing, showing that up to a bunch population of 8×10^{10} the beam is stable and giving the onset of the instability at about $10 - 12 \times 10^{10}$.

Finally, Fig. 6 shows the RMS bunch length, obtained with the simulation code, as a function of the bunch population up to an intensity of 2×10^{11} for the two bunch spacing cases.

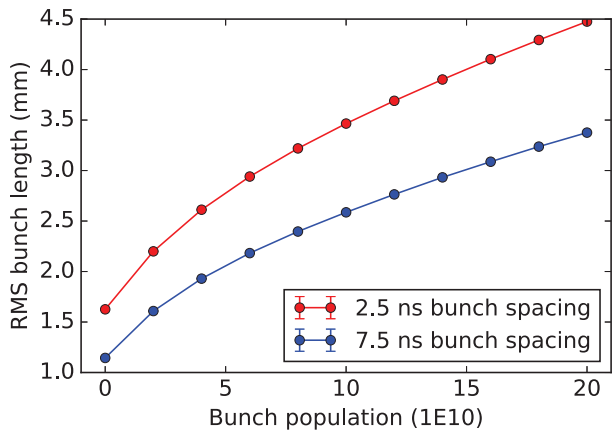

Figure 6: RMS bunch length as a function of bunch population as given by the simulation code with only the resistive wall impedance for 2.5 ns and 7.5 ns bunch spacing.

Multi-bunch Effects

A more critical situation is related to the transverse coupled bunch instability due to the long range transverse wake fields. In this case the study can be performed by considering the motion of the entire beam (not of the single bunch) as a sum of coherent oscillation modes, with coupled bunch

ISBN 978-3-95450-187-8

modes to be taken into account. By considering the lowest azimuthal mode $m = 0$ and a Gaussian bunch, the real part of the coupling impedance can produce stability or instability depending on the sign of the growth rate

$$\alpha_{\mu,\perp} = -\frac{cI}{4\pi(E_0/e)Q_\beta}\sum_{q=-\infty}^{\infty} Re\left[Z_\perp\left(\omega_q\right)\right] G_\perp\left(\sigma_\tau\omega'_q\right) \tag{10}$$

where I the total beam current, Q_β the betatron tune, σ_τ the RMS bunch length in time, $G_\perp$ a form factor which, for our case, is about 1, and

$$\omega_q = \omega_0\left(qN_b + \mu + Q_\beta\right) \qquad \omega'_q = \omega_q + \omega_0\xi\frac{Q_\beta}{\eta} \tag{11}$$

with N_b the number of bunches, ξ the chromaticity, and ω_0 the revolution frequency.

In the above equations, μ represents the μ^{th} coupled bunch mode, which goes from 0 to $N_b - 1$. When α_μ is positive, the corresponding mode is unstable. If we consider, as transverse impedance, the resistive wall one given by eq. (2), and ignore the term $-ib^4\omega^2$, we observe that $Re\left[Z_\perp\left(\omega\right)\right]$ depends on the sign of the frequency ω. Negative frequencies produce unstable modes with an exponential growth given by eq. (10), while positive ones give rise to damped oscillations. In addition to that, the resistive wall impedance grows approximately with the inverse of the square root of the frequency, determining the most dangerous coupled bunch mode when ω_q is as close to zero as possible. If we consider, as an example, the parameters given by Table 1 for the lowest energy and 2.5 ns bunch spacing, with $q = -1$, by denoting with Q_0 the integer part of the betatron tune, that is $Q_\beta = Q_0 + \nu_\beta$, with ν_β the fractional part of the tune, which plays a crucial role for this kind of instability, it comes out that the most dangerous coupled bunch mode is $\mu = N_b - Q_0 - 1 = 89949$, and this mode has its lowest negative frequency at $\omega_q = -\omega_0\left(1 - \nu_\beta\right)$.

Fig. 7 shows the beam spectrum of three coupled bunch modes and the real part of the resistive wall impedance of a circular pipe of aluminium, with radius of 35 mm and three layers, close to zero frequency for two extreme cases of fractional part of the betatron tune, $\nu_\beta = 0.05$ (red lines) and $\nu_\beta = 0.95$ (black lines), and we see that a smaller fractional tune is preferred to alleviate the transverse coupled bunch instability because the impedance has a lower value. Due to dynamic aperture and beam-beam issues, and since FCC-ee has 2 interaction points, the fractional tunes are indeed just above the integer [24], and therefore its fractional part is close to zero, mitigating the instability growth rate.

If we consider, as an approximation, not a sum of the impedance over frequency in eq. (10), but the coupling with a single betatron frequency line of the coupled bunch modes, the most dangerous unstable mode has a growth rate given approximately by

$$\alpha_\perp = \frac{cI}{4\pi(E/e)Q_\beta}\frac{C}{2\pi b^3}\sqrt{\frac{CZ_0}{\pi|1-\nu_\beta|\sigma_c}} \tag{12}$$

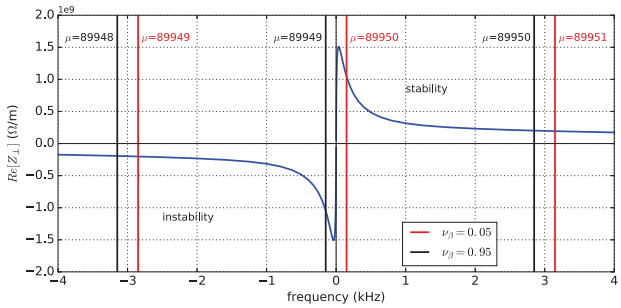

Figure 7: Coupled bunch spectrum and real part of the resistive wall impedance as a function of frequency around $f = 0$ for fractional tune $\nu_\beta = 0.05$ (red line) and $\nu_\beta = 0.95$ (black line).

which, for the best case with $\nu_\beta = 0.05$, gives a growth rate of about 432.4 s^{-1}, corresponding to a rise time of approximately 2.3 ms, that is about 7 machine turns. If the fractional tune increases, the situation worsens because the most dangerous spectrum line couples a higher impedance.

A more precise calculation by considering the sum in eq. (10) and by using the Laguerre polynomials with the DELPHI code confirms the values of the growth rates. Even if the rise times are in the range of few milliseconds, which are not typically a concern for an accelerator machine, due to the large circumference, the rise times correspond to very few turns, making very challenging the realization of a feedback system. Some schemes that could deal with this problem have been proposed in ref. [25].

For what concerns possible longitudinal coupled bunch instabilities excited by HOMs, at this stage it is not possible to quantify their impedance contribution, but we can estimate the maximum shunt impedance giving a growth rate that can be compensated by the natural radiation damping.

Similarly to the transverse case, by considering only the lowest longitudinal azimuthal mode $m = 1$, it is possible to show that the real part of the HOM impedance can produce stability or instability depending on the sign of the growth rate

$$\alpha_{\mu,||} = \frac{\eta I}{4\pi\left(E_0/e\right)Q_s}\sum_{q=-\infty}^{\infty}\omega_q Re\left[Z_{||}\left(\omega_q\right)\right] G_{||}\left(\sigma_\tau\omega_q\right) \tag{13}$$

with Q_s the synchrotron tune and $\omega_q = \omega_0(qN_b + \mu + Q_s)$. Stability in this case occurs for negative frequencies because the real part of the longitudinal impedance is always positive, and the worst and simplest unstable case is when the HOM has its resonant angular frequency ω_r equal to $\omega_q > 0$. If we consider, as an approximation, not a sum of the impedance over frequency, but the coupling with a single synchrotron frequency line of the coupled bunch modes, the most dangerous unstable mode has a growth rate given approximately by

$$\alpha_{||} = \frac{\eta I}{4\pi\left(E_0/e\right)Q_s}\omega_r R_s \tag{14}$$

ISBN 978-3-95450-187-8

with R_s the HOM shunt impedance. Also in this case $G_{||}(x) \simeq 1$, if $f_r \ll 25$ GHz. This growth rate has to be compared with the natural damping rate due to the synchrotron radiation, which, for the lowest energy machine, is about 1320 turns. In Fig. 8, we have represented the maximum HOM shunt impedance of eq. (14) as a function of the resonance frequency, such that the corresponding growth rate is exactly balanced by the radiation damping. Of course, also here a feedback system has to be developed as a further safety knob.

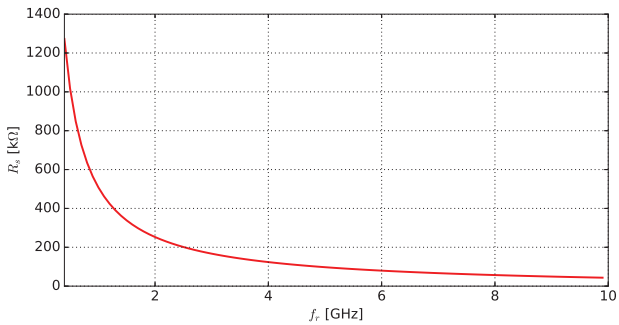

Figure 8: Maximum shunt impedance of a HOM as a function of its resonance frequency, producing a growth rate that is compensated by the natural radiation damping.

OTHER IMPORTANT IMPEDANCE SOURCES

In the previous section, by discussing the effects of the resistive wall, we have seen that its impact on the beam dynamics is very important, requiring, in some cases, active feedback systems to keep under control beam instabilities. In addition to that, other machine devices can be sources of high impedance, and their evaluation is paramount.

Let us first estimate the impact of the synchrotron radiation absorbers. For FCC-ee a synchrotron radiation absorber will be installed every 4-6 meters, with the purpose of intercepting the radiation that, otherwise, would impact on the beam chamber. Due to their large number, the absorbers represent a very important source of machine impedance.

A proposed design foresees a modification of the circular pipe with winglets on both sides, as the one of SuperKEKB [26].

The absorbers are metallic devices shaped like a trapezoid, with a total length of 30 cm, and they are inserted inside the chamber winglets, at about 42.5 mm from the beam axis. Placing slots for vacuum pumps just in front of the absorber allows efficient capturing of the synchrotron radiation and the molecule desorption. The pumping slots have a racetrack profile, length of 100-120 mm and width of 4-6 mm. Behind the slots, a cylindrical volume and a flange will be installed to support a NEG pump [27].

Impedance studies of the beam chamber profile with one absorber insertion have been performed using CST Particle Studio [28]. In Fig. 9, the geometry of the FCC-ee beam chamber used in CST simulations is shown together with a detail of the absorber inside the beam chamber. Pumping slots and pumps are not included in this simplified model. Preliminary simulations show that below about 3 GHz the longitudinal impedance is purely inductive, giving, for 10000 elements, a longitudinal broadband impedance Z/n of about 1 mΩ.

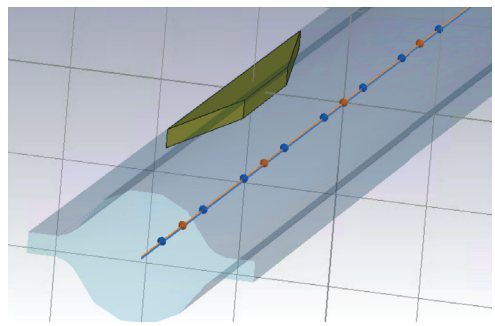

Figure 9: 3D model of the FCC-ee vacuum chamber with winglets and a synchrotron radiation absorber used for CST simulations.

In Fig. 10, the wake potentials for 2 and 4 mm Gaussian bunches for 10000 elements are shown. Even if further analysis is needed, and this first evaluation could overestimate the impedance, we can see that these wake potentials are not negligible. As for the transverse impedance of a single absorber, this is so low that, up to now, we did not manage to obtain reliable results.

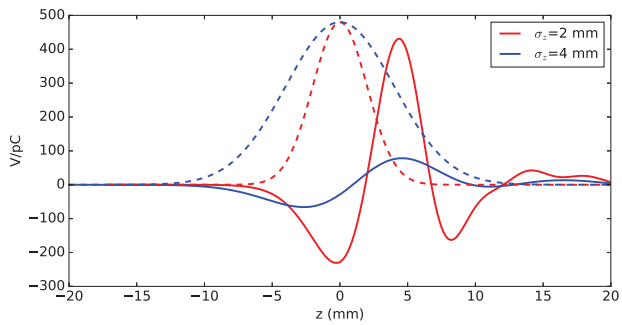

Figure 10: Wake potential of 10000 abosorbers for 2 and 4 mm RMS bunch length from CST code.

In FCC-ee there will be many straight sections used for installation of RF systems, quadrupoles with attached BPMs, diagnostics etc. Due to the particular shape of the dipole vacuum chambers with winglets, gradual transitions (tapers) are to be foreseen to connect these chambers to the circular pipes of the straight sections. A possible design of such transitions is shown Fig. 11. The total number of double tapers is estimated to be around of 4000. Their total longitudinal wake potentials for 2 mm and 4 mm bunch lengths are shown in Fig. 12.

ISBN 978-3-95450-187-8

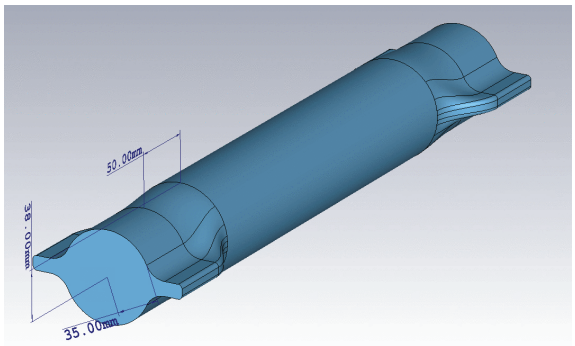

Figure 11: Taper connecting the vacuum chamber with winglets to the circular pipe.

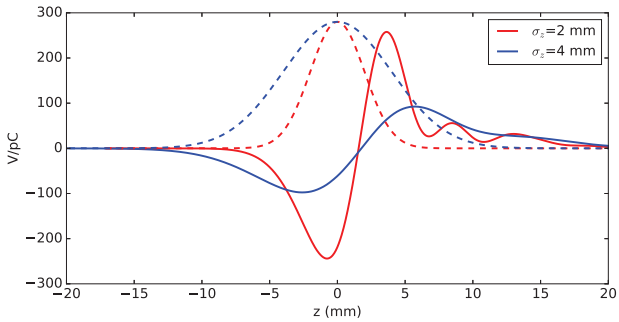

Figure 12: Wake potential of 4000 double tapers for 2 and 4 mm RMS bunch length from CST code.

The RF system is another important source of the beam coupling impedance. Several options of the system are under investigation [29]. For our study we consider the use of 100 single cell 400 MHz cavities, similar to those used in LHC. We assume that, like in LHC, these cavities are separated in groups composed of 4 cavities, placed in common cryostats and connected by tapers to the beam pipe. As a consequence, in addition to the 100 single cell cavities, also the impedance contribution of 25 double tapers has to be taken into account. The wake potentials for the single cells have been obtained with the ABCI code [30], and the results can be very well approximated by the analytical expression [3]

$$W(x) = \tilde{W}|x|^{1/4}e^{-x}\left[I_{-1/4}(x) + \mathrm{sign}(z)I_{1/4}(x)\right] \qquad (15)$$

with $x = [z/(2\sigma_z)]^2$ and $\tilde{W} = 1.92 \times 10^6/\sqrt{2\pi\sigma_z/c}$.

The impedance produced by the tapers strongly depends on their length, which we have considered here to be 500 mm. The wake potential of the total RF system under these assumptions is shown in Fig. 13.

If we consider the longitudinal wake potentials of the absorbers, the smooth transitions and the RF system, we see that their sum cannot be neglected with respect to the resistive wall. Even if the contribution of a single element is negligible, due to their high number, the effect on the beam dynamics could be important. In Fig. 14 we show the total wake potential for 2 mm and 4 mm bunch lengths, given by the contributions evaluated so far. We can see that there has been an increase of about 50% with respect to the resistive

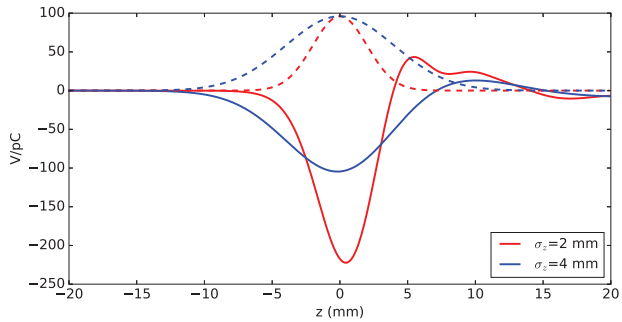

Figure 13: Wake potentials of the RF system for 2 and 4 mm RMS bunch length.

wall contribution. Beam dynamics studies are in progress to evaluate the impact of such wakes on coherent instabilities.

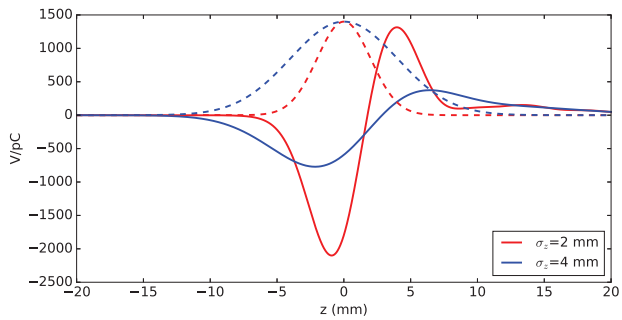

Figure 14: Total wake potentials for 2 and 4 mm RMS bunch length given by the contributions of resistive wall, synchrotron radiation absorbers, RF system and tapers.

Of course, also the transverse contribution of the previous devices has to be taken into account to determine the impact of the impedance on the TMCI. In addition, there are several other sources of impedance, such as the bellows, RF fingers, BPMs and other devices for diagnostics, and their impact on beam dynamics has to be carefully evaluated. Also possible trapped modes in the interaction region deserve special studies, and work on other collective effects, such as the fast ion and the electron cloud instabilities, is in progress.

CONCLUSIONS AND OUTLOOK

In this paper we have discussed single beam collective effects in FCC-ee due to the beam coupling impedance. In particular we focused our study primarily on the resistive wall effects because this is, up to now, the main source of impedance.

We have found that, in the single bunch case, the transverse mode coupling instability threshold due to the resistive wall is by about a factor 6 higher than the nominal bunch population at the lowest energy (45.6 GeV) for 2.5 ns bunch spacing, and even higher for other collider energies. In turn, the microwave instability threshold has a safety margin of 2.4 with respect to the nominal bunch population for the 2.5 ns bunch spacing, while for the 7.5 ns option the threshold is equal to the nominal bunch intensity. Besides, the resistive

ISBN 978-3-95450-187-8

wall results in the bunch shape distortion and substantial bunch lengthening (see Fig. 4 and Fig. 6).

Regarding the multi-bunch effect, we have concluded that the resistive wall transverse coupled bunch instability has to be counteracted by a feedback system, which requires innovative ideas for its design. For the longitudinal case, at this stage, it is not possible to evaluate the characteristics of trapped HOMs, but an estimate of the maximum allowed shunt impedance as a function of the resonant frequency has been given.

In addition to the assessment of the resistive wall effects, we have started the evaluation of the impedance budget for other devices, with the goal of designing them in order to reduce their impact on the beam dynamics. With an accelerator of 100 km of length, this is a long work, and the strategy is to identify the most important sources of impedance. We have started with the synchrotron radiation absorbers, the RF system, and smooth transitions from the beam pipe with winglets to the circular one. The results show that the total wake potential is increased of about 50% with respect to the resistive wall one.

ACKNOWLEDGEMENTS

We acknowledge many helpful and stimulating discussions with R. Calaga, R. Kersevan, K. Oide, E. Shaposhnikova, G. Stupakov, J. Wenninger, and F. Zimmermann.

REFERENCES

[1] The HiLumi LHC Collaboration, CERN-ACC-2014-0300, CERN, Geneva, Switzerland (2014).

[2] https://fcc.web.cern.ch/

[3] L. Palumbo, V. G. Vaccaro, M. Zobov, CERN 95-06, pp. 331-390, CERN, Geneva, Switzerland (1995), and arXiv: physics/0309023 LNF-94-41-P.

[4] F. Sacherer, IEEE Trans. Nucl. Sci. 20, 825 (1973); IEEE Trans. Nucl. Sci. 24, 1393 (1977).

[5] A. W. Chao, *Physics of Collective Beam Instabilities in High Energy Accelerators*, John Wiley & Sons, (1993).

[6] J. L. Laclare, CERN 87-03, Vol. I, p. 264, CERN, Geneva, Switzerland (1987).

[7] B. Zotter, CERN-SPS/81-18, 81-19, 81-20, (DI), CERN, Geneva, Switzerland (1981).

[8] C. Pellegrini, AZP Proc. 87, Phys. High Energy Part. Accel., Fermilab, p. 77 (1981).

[9] M. Sands, SLAC-TN-69-8, and SLAC-TN-69-10 (1969).

[10] see, e. g., T. Suzuki and K. Yokoya, Nucl. Instr. and Meth., 203, p. 45 (1982), or K. Y. Ng, *Physics of Intensity Dependent Beam Instabilities*, World Scientific, (2005).

[11] K. Y. Ng and K. Bane, SLAC-PUB-15078, (2010).

[12] K. Bane and M. Sands, SLAC-PUB-95-7074, (1995).

[13] E. Belli, M. Migliorati, S. Persichelli, M. Zobov, CERN-ACC-2016-0111 (2016), and arXiv:1609.03495 (2016).

[14] R. Kersevan, private communication.

[15] N. Mounet, Ph.D. thesis, École Polytechnique Fédérale de Lausanne (EPFL), Lausanne, Switzerland, 2012.

[16] M. Migliorati, L. Palumbo, Phys. Rev. ST Accel. Beams, 18, 031001 (2015).

[17] R. Boni, et al., NIMA 418, p. 241 (1998); M.Zobov et al., e-print: physics/0312072.

[18] M. Migliorati, et al., Phys. Rev. ST Accel. Beams, 16, 031001 (2013).

[19] A. Piwinski, DESY Report 72/72 (1972).

[20] J. Haïssinski, Il Nuovo Cimento, Vol. 18 B, N. 1, (1973).

[21] see, e. g., Y. Cai, Phys. Rev. ST Accel. Beams, 14, 061002 (2011).

[22] K. L. F. Bane, Y. Cai, and G. Stupakov, SLAC PUB -14150, June 2010.

[23] R. Warnock and J. Ellison, SLAC-PUB-8404, (2000).

[24] see, e. g. K. Oide, presentation at the FCC Week 2016 - 11 April 2016, Rome - https://indico.cern.ch/event/438866/contributions/1085096/attachments/1255571/1853343/Optics_KO_160411a.pdf

[25] see A. Drago, presentation at the FCC Week 2016 - 11 April 2016, Rome - https://indico.cern.ch/event/438866/contributions/1085137/attachments/1257184/1857470/Drago_fb_fcc_ee.pdf

[26] Y. Suetsugu eta al, *Design and construction of the SuperKEKB vacuum system*, J. Vac. Sci. Technol. A 30, 031602 (2012).

[27] R. Kersevan, Proceedings FCC Week 2016 - 14 April 2016, Rome - https://indico.cern.ch/event/438866/contributions/1085121/

[28] https://www.cst.com/

[29] S. Aull, et al., Proceedings of IPAC2016, Busan, Korea, p. 3828 (2016).

[30] Y. H. Chin, KEK Report 2005-06, KEK, Tsukuba, Japan (2005).

ISBN 978-3-95450-187-8